Water in the Landscape: A Review of Contemporary Flow Routing Algorithms

John P. WILSON, Graeme AGGETT, DENG Yongxin and Christine S. LAM

Abstract

This chapter reviews the various flow routing algorithms that simulate the distribution and flow of water across landscapes. The distinguishing characteristics of nine such algorithms and the experiments that have been conducted to evaluate their performance over the past 15 years are discussed. From there, we consider three sets of enduring challenges: (1) the role of scale and feedback between soil and water, and the need to consider these issues when characterizing the properties of both; (2) the need for dynamic flow routing algorithms and related indices in many landscapes; and (3) some of the as yet unrealized opportunities for treating space and time as continuous variables in the representation of soil water properties. The chapter concludes by noting the current state-of-the-art and where we might go from here.

Keywords: DEMs, flow routing algorithms, soil water relationships.

1 Introduction

A growing body of literature from the 1990s illustrates how flow routing measurements and related topographic attributes can be used in modelling key hydrologic processes controlling the spatial distribution of soil moisture, runoff, and soil erosion in a simplified but realistic manner (e.g. Band 1989, Moore *et al.* 1993, Abbott and Refsgaard 1996, Cluis *et al.* 1996, Maidment 1996, Da Ros and Borga 1997, Beven 1998, Storck *et al.* 1998). The identification of drainage pathways and runoff contributing areas based on DEMs, together with their coupling with hydrological models (e.g. Beven *et al.* 1994, Lee and Chu 1996), provides the means to parameterize spatially distributed, physically-based models, which themselves represent a major approach for incorporating spatial heterogeneity. Digital terrain analysis provides a quantitative and consistent approach to generating inputs for applications of these models as discussed below.

The elevation, slope, and aspect of an area have a strong influence on its microclimate due to insolation and other effects, and topography has a major impact on the hydrological, geomorphological, and biological processes active in landscapes (Moore *et al.* 1993, Dymond *et al.* 1995, Cluis *et al.* 1996, Pickup and Chewings 1996). Geomorphometric parameters derived from DEMs can be used to determine where in a watershed various slope processes, such as landslides and runoff, take place (Montgomery *et al.* 1998). At the local scale, primary geomorphometric parameters can be extracted using standard GIS tools in order to investigate morphometric influences on hydrologic variables such as overland flow depth and velocity. For example, the widely used hydrologic model TOPMODEL is based on the concept of variable source areas contributing to runoff production through saturated overland flow (Beven *et al.* 1994). Formation of the contributing area is related to the topographic index $\ln(A_s/\tan\beta)$, where A_s is the upslope area drained per unit contour length and β is the slope angle. Model inputs are the frequency distribution of $\ln(A_s/\tan\beta)$, daily precipitation and evapotranspiration time series, and several lumped soil and flow routing parameters. Model outputs include the runoff hydrograph, water balances, and contributing areas. Developments in hydrologic models have been greatly facilitated by GIS, which supports the spatial data models that have enabled earth scientists to construct more distributed representations of space than previously possible. Using GIS to parameterize such models has enabled their application across local, watershed, and regional scales, facilitating more realistic model assessment and more accurate process modelling.

The strong influence of elevation and watershed morphology on precipitation, water movement, and slope stability means that DEMs serve as one of the basic building blocks of many environmental model parameterization efforts, and the enhancements made to flow routing measurements have enhanced this capacity. The increasing availability of DEMs, remotely-sensed data, and a dramatic increase in desktop computing power over the past decade have accelerated these developments, enabling researchers to link their chosen process-based model(s) to a spatial database contained within a GIS.

This chapter reviews the most popular flow routing algorithms and what is known about their performance. The choice of algorithm is critical given the key contribution of water distribution and flow in soil development, land cover, soil redistribution, and various forms of mass movement. The remainder of this chapter is divided into three sections. The distinguishing characteristics of nine such algorithms – the D8 (O'Callaghan and Mark 1984), Rho8 (Fairfield and Leymarie 1991), FD8 (Quinn *et al.* 1991), Lea (1992), DEMON (Costa-Cabral and Burgess 1994), ANSWERS (Beasley and Huggins 1978), flux decomposition (Desmet and Govers 1996), D∞ (Tarboton 1997), and MFD-md (Qin *et al.* 2007) algorithms – are first outlined. We then review the continued importance of source data, interpolation algorithms, and the experiments that have been conducted to evaluate their performance over the past 15 years in Section 3. Three groups of studies – those focused on inputs and/or decision rules and those focused on the ability of one or more of the aforementioned algorithms to reproduce the drainage structure or some relevant landscape properties with and without the assistance of field observations – are discussed. The last section concludes by noting the current state-of-the-art and where we might go from here.

2 Basic Characteristics of Flow Routing Algorithms

The automated extraction of surface channel networks from DEMs has grown in popularity during the past 20 years as the availability and resolution of DEMs, as well as the quality of hydrologic modelling tools, has improved. Identifying channel networks and their initiation points is central to hydrology and geomorphology because of the control exerted by climate, topography, soil properties, and other environmental attributes on surface flow paths and erosion potential within a drainage basin (Knighton 1998). The characteristics of a channel network heavily depend on the identification of channel source cells from the digital landscape, and can greatly affect the delineation of catchments or drainage basins (Garbrecht *et al.* 2001). The closer the channels begin to the drainage divide, the greater the number of channels that can occupy a watershed (Montgomery and Dietrich 1988). DEMs generally cannot capture all topographic variations that occur within the landscape, especially if the features are finer than the DEM resolution, and these shortcomings may cause discrepancies between the precise positioning of stream channels in digital landscapes and the real world (Garbrecht *et al.* 2001).

Flow routing algorithms have been used to predict the channel source cells as well as the movement of water, sediment, and nutrients to lower adjacent points or areas in a landscape (e.g. Desmet and Govers 1996). Fundamentally, a flow routing algorithm determines the way in which the outflow from a given cell will be distributed to one or more neighbouring downslope cells. The choice of flow routing algorithm is important as it affects the calculation of the upslope contributing area, the prediction of flow accumulation, and several other topographic and hydrologic attributes. The derivation of these attributes relies on digital elevation source data. Square-grid DEMs are a popular choice for flow routing due to their visual simplicity and ease of computer implementation (Moore *et al.* 1991, Wise 1998a, b, Wilson and Gallant 2000). All nine of the flow routing algorithms discussed below utilize square-grid DEMs as their primary input data, and calculate flow directions and upslope contributing areas using a 3 x 3 moving window.

The D8 (deterministic eight-node) single-flow-direction (SFD) algorithm directs flow from each grid cell to one of eight nearest neighbours based on slope gradient (O'Callaghan and Mark 1984). The aspect Ψ (measured in degrees clockwise from north) marks the direction of steepest descent for each grid cell or point in a catchment, and is the direction in which water would flow from that grid cell or point. Most implementations of D8 utilize the primary flow direction for water moving over the land surface as an approximate replacement for aspect (Moore 1996). The simplest method of calculating primary flow direction is to determine the slope (S_i) to each neighbour and set it to the direction for which S_i is greatest (Gallant and Wilson 2000). The upslope contributing area is the number of cells whose flow reaches the cell of interest multiplied by the cell area, while specific catchment area is the upslope contributing area divided by the contour width, which is assumed to equal the "width" of a grid cell. Some implementations of D8 utilize the grid spacing for both cardinal and diagonal flow assignments, while others, such as TAPES-G (Gallant and Wilson 1996), assume that the grid cell width is a good estimate for flow width in the cardinal directions and that the cell width multiplied by √2 is the best estimate of the flow width for flow assignments to diagonal cells. However, there is little theoretical or empirical evidence to support either option (Gallant *et al.* 2000).

The Rho8 (random eight-node) SFD algorithm developed by Fairfield and Leymarie (1991) introduced a degree of randomness to break up the parallel flow paths that D8 tends to produce on planar surfaces (Wilson and Gallant 2000). This algorithm starts by identifying all the neighbouring downslope cells, then calculates the slope gradients in each of these directions, and finally extracts random numbers from a table to direct the flow to one of these candidate cells. The random numbers are allocated on a slope-weighted basis such that the potential flow paths with the steepest gradients have the greatest probability of being selected, and the overall flow pattern more or less matches the one produced with D8. The upslope contributing and specific catchment areas are calculated using the flow width and flow accumulation approaches adopted for D8; however, a different flow network will be produced each time the algorithm is used because of the random assignment of flow among multiple downslope cells (Wilson *et al.* 2000).

The FD8 multiple flow direction (MFD) algorithm developed by Quinn *et al.* (1991) directs water to every adjacent downslope cell on a slope-weighted basis. The slope gradients, slope lengths, and two weights – 0.5 and 0.35 for cardinal and diagonal directions, respectively – are used to direct the flow from the centre cell to each downslope cell in a 3 x 3 moving window. Each cell receives a fraction of the discharge from each upslope cell, and therefore, the upslope contributing area of the receiving cell is typically composed of partial contributions from many different cells. Specific catchment area is calculated as the sum of the contributing areas from upslope cells divided by the cell width for the cardinal flow directions, and by the cell width multiplied by √2 for diagonal flow directions (similar to D8 and Rho8 in TAPES-G). The user can set a maximum cross-grading area threshold in the TAPES-G implementation of FD8 to switch to the D8 algorithm. This approach means that flow dispersion will be terminated whenever the upslope contributing area exceeds this user-specified threshold (Gallant and Wilson 1996, Wilson and Gallant 2000).

Lea's (1992) flow routing algorithm relies on the calculation of the aspect vector and a surface fitting scheme. He argued that flow moves across a planar surface in the direction of the steepest slope, or aspect angle θ, similar to a "rolling ball". The approach has two parts. First, planes are constructed to represent the surface of each cell using estimated elevations at the four corners of each cell. Successively larger windows can be implemented to minimize the occurrence of flat areas (i.e. surface pits). The aspect vector is calculated during the second step in 1° increments (in contrast to the 45° increments used for many implementations of D8) and is utilized to route flow across individual cells. Flow paths are constructed by the repeated application of the algorithm until the catchment outlet is reached or a topographic hollow prevents the continued progress of flow. The contributing area is calculated as the number of flow paths passing through that cell multiplied by the grid cell area, and an arbitrary threshold is utilized to dictate the number of flow paths that need to converge on a pixel for it to be classified as a stream path.

The fifth algorithm called DEMON (Digital Elevation Model Network) was developed by Costa-Cabral and Burgess (1994) and determines flow direction based on the local aspect angle similar to Lea (1992). However, the flow generated over a cell is directed downslope over a two-dimensional flow strip. These flow strips partition catchments into irregularly shaped elements that are defined by pairs of orthogonals and equipotential lines (contour lines). The width of the flow strips increases over divergent topography, decreases over convergent topography, and remains constant over planar surfaces. The flow across each cell is the amount of flow entering that cell plus the flow generated by the cell itself. When flow reaches an edge of a grid cell at a cardinal direction, then all flow is directed to the single neighbour. In other cases, the flow is split amongst the cardinal neighbours. The upslope contributing area for each cell in DEMON is computed by successive addition of the cell areas in each stream tube entering every pixel in the DEM, and the specific catchment area is computed by dividing the upslope contributing area by the flow matrix width. A modified version of DEMON is implemented in TAPES-G in which the nodes of the DEM define the centre of the cells instead of the entire cell area, and the flow direction of a stream tube is defined by the aspect. The upslope contributing and specific catchment areas are calculated in the same way as in the original version of DEMON in TAPES-G (Gallant and Wilson 2000).

The ANSWERS (Areal Nonpoint Source Watershed Environment Response Simulation; Beasley and Huggins 1978) non-point source pollution model describes the runoff, infiltration, subsurface drainage, erosion, and drainage across a watershed during and following single storm events. The watershed is divided into grid cells with parameters provided for each cell, and the continuity equation is used with a stage-discharge curve to calculate the amount of flow that would cross each cell. The cells are split into two parts by a line through one of the cell corners and oriented in the aspect direction of the cell, and the relative proportions used to divide and direct the flow of water into the neighbouring downslope cardinal cells. This algorithm was implemented as a FORTRAN program and coupled with IDRISI (Eastman 1992) by Desmet and Govers (1996) as part of a study comparing the performance of flow routing algorithms in a small catchment near Flanders, Belgium. Two modifications were made to the original ANSWERS algorithm by Desmet and Govers (1996) to solve specific problems such that: (1) flow was assigned to just one of the two cardinal cells when flow was directed to grid points of equal or even higher height; and (2) flow was switched to the D8 steepest descent algorithm (i.e. the diagonal path in a 3 x 3 moving window) when both of the two receiving cells were higher than the central point.

Desmet and Govers (1996) also proposed a new flow routing algorithm based on the decomposition of the flux vector. The flux vector was split into two ordinal components with the magnitude of each component proportional to the sine or cosine of the aspect value. The magnitudes of the two components were normalized by dividing each by the sum of the absolute values of the sine and cosine of the aspect value, and the two modifications noted above for the ANSWERS flow routing algorithm were adopted as a part of this algorithm as well. This algorithm splits the upslope contributing area between two cardinal neighbours and the calculation of specific catchment area is similar to that of D8, FD8 and Rho8 in

TAPES-G, where the contributing area is divided by the effective contour length. The major difference between the ANSWERS and flux decomposition algorithms concerns the routing of flow to the two cardinal neighbours. Beasley and Huggins (1978) chose to divide grid cells based on which cardinal neighbour received flow lines parallel to the aspect direction, whereas Desmet and Govers (1996) relied on the sine and cosine of the aspect vector values to direct flow to these candidate cells.

The D∞ algorithm proposed by Tarboton (1997) incorporates several ideas from DEMON to assign multiple flow directions to selected cells. The flow direction follows the path of steepest descent and is represented as a continuous angle between 0 and 2π radians. Special rules are included to: (1) force flat cells to drain to a neighbour that ultimately drains to a lower elevation; and (2) eliminate loops in the flow direction angles. Grid cells that are flat took flow direction from the D8 method in the original D∞ code, but the latest version uses the method of Garbrecht and Martz (1997) to assign flow directions in flat areas. This algorithm returns NODATA for flow direction in grid cells classified as pits. The upslope area of each cell is taken as its own area plus the fractional areas of upslope neighbours that drain into the cell of interest, similar to FD8 and DEMON. If the angle falls on a cardinal or diagonal direction, then the flow from each cell drains to one neighbour. If the flow direction falls between the direct angles to two adjacent neighbours, the flow is apportioned between the two cells according to how close the flow direction angle is to the direct angle for those cells.

The final MFD-md algorithm proposed by Qin *et al.* (2007) utilizes local topographic conditions to partition the flow between downslope neighbouring cells. This algorithm modifies the flow partition approach of Quinn *et al.* (1991) by utilizing the maximum downslope gradient to model the impact of local terrain on the flow partitioning predicted at each cell. The maximum slope gradient was chosen for inclusion in this algorithm over the minimum and mean downslope gradients because: (1) it is less sensitive to variations in DEM error; and (2) the new algorithm will behave like D8 in steep terrain (Qin *et al.* 2007). The MFD-md flow partitioning scheme uses an exponent that takes values between 1.1 and 10 to model divergent (small flow partition exponent values) and convergent flow (large exponent values) across the landscape (similar to the schemes proposed by Freeman 1991, Holmgren 1994, and Quinn *et al.* 1995).

This proliferation of flow routing algorithms raises an important question; namely, whether one or more of these algorithms performs better than the others in specific landscapes and/or applications. Figure 1 builds on the approach of Qin *et al.* (2007) and shows the routing of flow from the centre cells in three hypothetical DEMs to one or more downslope neighbours for the nine aforementioned flow routing algorithms. These relatively simple examples show how different flow routing algorithms can generate substantially different estimates of upslope contributing area and related attributes (specific catchment area, topographic wetness index, etc.). The major findings from published studies comparing the performance of two or more of these flow routing algorithms are taken up and discussed in more detail below.

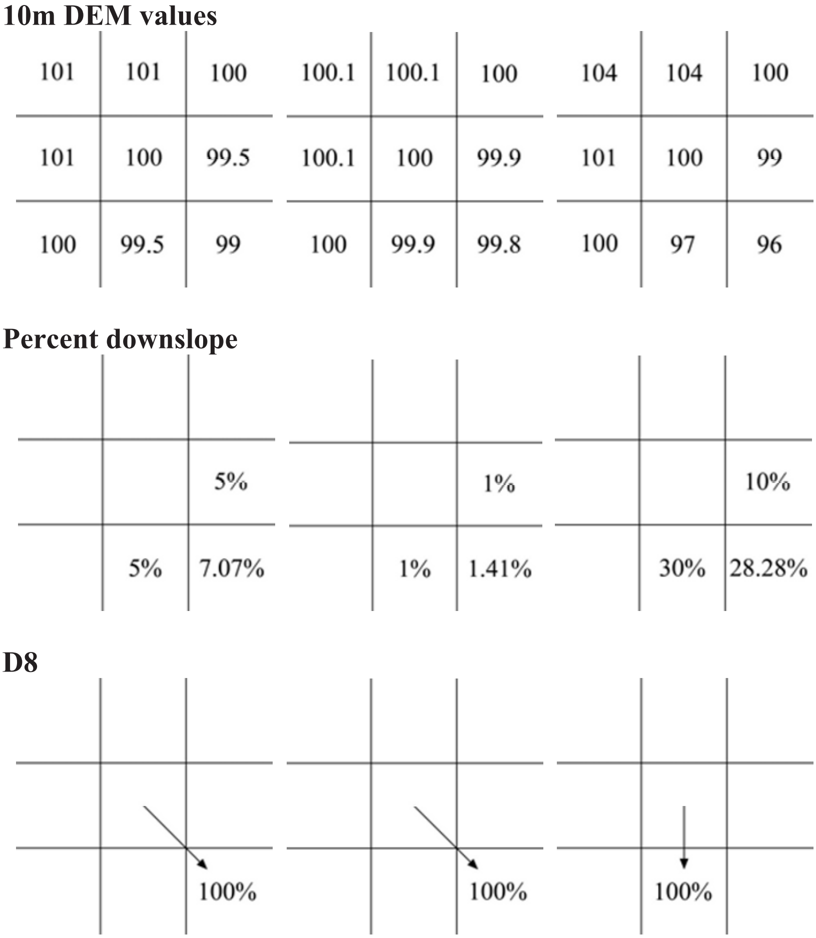

Figure 1. Flow partitioning schemes for nine flow routing algorithms and the three sample DEMs.

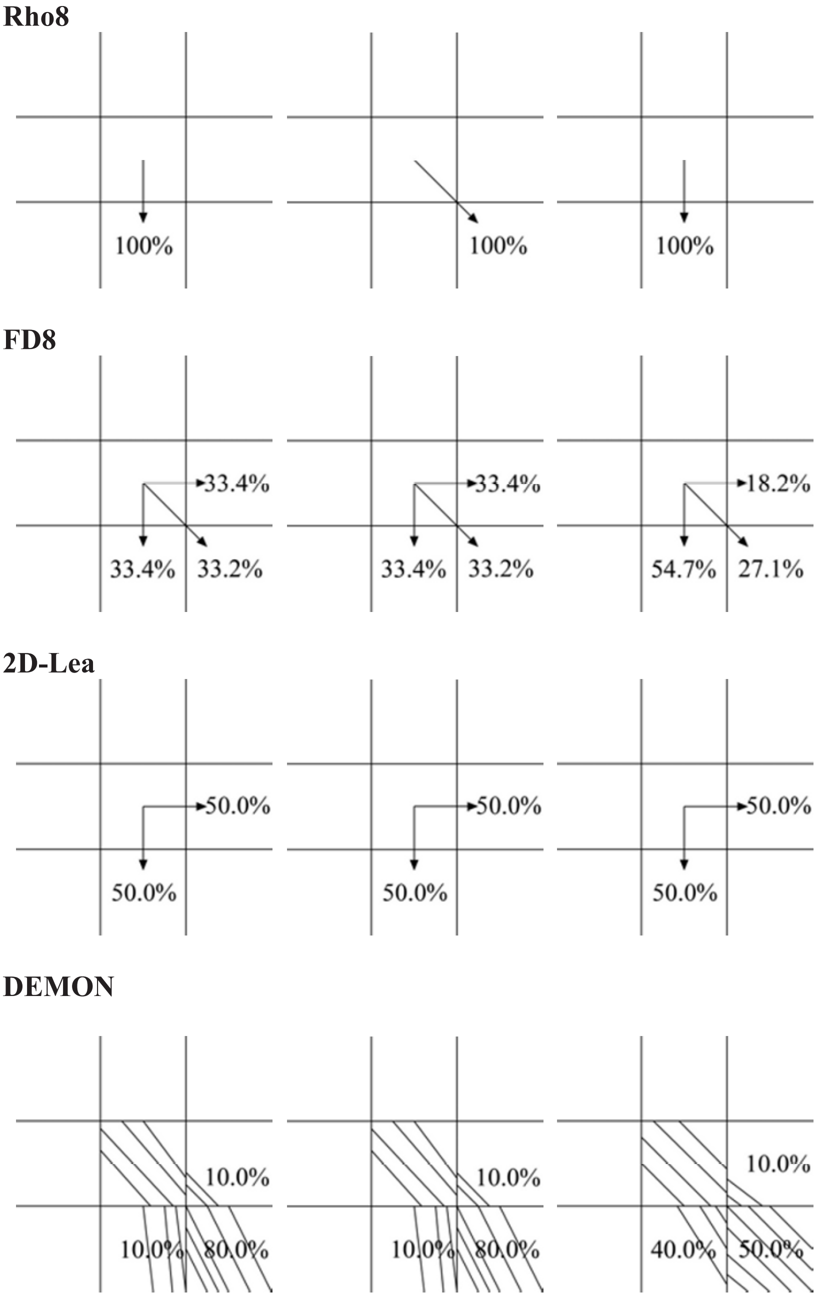

Figure 1. (Continued)

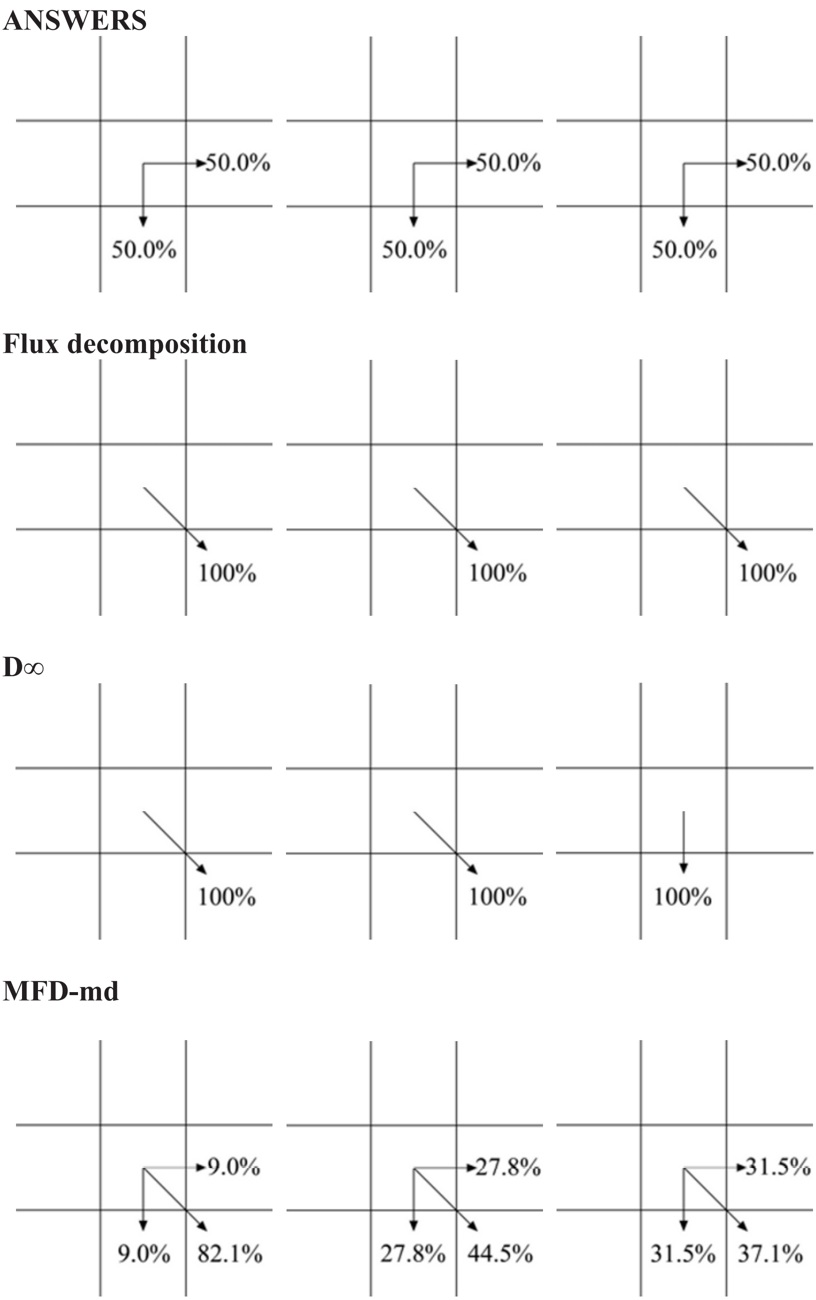

Figure 1. (Continued)

3 Comparisons of Flow Routing Algorithms

The evaluation of flow routing algorithm performance is tricky because of the importance of the underlying source data and the difficulty of separating the impact of the flow routing algorithms from that of the underlying data when reviewing their performance. The elevation data may take one of three forms (square-grid, triangulated irregular, and contour-based networks) although the proliferation of digital elevation sources and preprocessing tools means that the initial choice of data structure is not as critical as it once was (Kemp, 1997a, b). Numerous methods have been proposed to convert digital elevation data from one structure to another, but care must still be exercised with each of these methods to minimize unwanted artefacts (e.g. Krajewski and Gibbs 1994).

Hutchinson (2007) recently documented a 20-year trend of shifting spatial scales – from continental and regional scales (e.g. major drainage divisions), to the mesoscale (e.g. surface climate), and then to the toposcale (e.g. soil properties) – in hydro-ecological applications of topographic data. These scale transitions have mirrored advances in DEM resolutions and improvements in representing local terrain shape and structures. This focus on local details has allowed landforms and hydrological patterns to be differentiated within small watersheds (e.g. 1–100 km^2 in size) and hillslopes (e.g. 100–1,000 m in length). However, larger quantities of data do not necessarily produce better results: Eklundh and Martensson (1995), for example, used ANUDEM (Hutchinson 1989) to derive square grids from contours and demonstrated that point sampling produces faster and more accurate square-grid DEMs than the digitizing of contours. Similarly, Wilson *et al.* (1998) used ANUDEM to derive square grids from irregular point samples and showed that many of the x, y, z data points acquired with a truck-mounted GPS were not required to produce satisfactory square-grid DEMs. ANUDEM calculates ridge and streamlines from points of maximum local curvature on contour lines and incorporates a drainage enforcement algorithm that automatically removes spurious sinks or pits in the fitted elevation surface (Hutchinson 1989). ANUDEM is one of several programs of this type (see Maidment 1996 and Hellweger 1996 for other examples) that modify a DEM to reflect known hydrology, and there are many other methods that have been proposed over the years to automatically extract drainage networks and ridgelines from digital elevation data (e.g. Qian *et al.* 1990, Smith *et al.* 1990).

This proliferation of digital elevation data sources and preprocessing tools is to some extent problematic given the task at hand. Carrara *et al.* (1997), for example, compared several methods for generating DEMs from contour lines and concluded that the range of terrain types, sample structures, and modelling routines is so great that attempts to make generalizations about "best" models is tremendously difficult. Similarly, Callow *et al.* (2007), for example, examined three different algorithms that modify a DEM to reflect known hydrology and showed that these methods permanently altered the source DEM and a variety of computed topographic attributes. Some of the interpolation methods that have been proposed are difficult to use and as a consequence Eklundh and Martensson (1995) recommended that less experienced users focus on the quality of the input data instead of learning sophisticated interpolation methods. Simpler interpolation methods will give satisfactory results so long as the input data are well sampled and sophisticated algorithms are likely to produce unsatisfactory results if applied to poor data (e.g. Wilson *et al.* 1998).

It is perhaps not surprising given this background that many modellers accept the DEMs they work with uncritically despite an ever-increasing literature describing the causes of systematic and random errors in DEMs, and their effects on morphometric and hydrologic parameter estimation (e.g. Lagacherie *et al.* 1996, Lopez 1997, Murillo and Hunter 1997, Wise 1998a, b). If undetected and uncorrected they may propagate into the process models they are used to parameterize, causing considerable uncertainty in the reliability of their simulations. Small errors in elevation or strange behaviour by an interpolator can produce large errors in surface derivatives such as gradient, and topographic surfaces used to define boundary conditions in environmental modelling applications will contain error (Desmet 1997, Liu and Jezek 1999).

Numerous studies have attempted to evaluate the performance of two or more flow routing algorithms notwithstanding the complications introduced by the choice of source data and/or interpolator and the presence of systematic and/or random errors. These studies can be grouped into three sets and their results are discussed in some detail below. The first two studies have examined the sensitivity of flow routing predictions to one or more of the decision rules embedded in the chosen flow routing algorithms.

Wilson *et al.* (2000) examined the effect of DEM source, grid resolution, and choice of flow routing algorithm on three primary and two secondary topographic attributes for a large forested catchment in southwest Montana. The comparisons showed that the D8 and Rho8 SFD algorithms initiated flow from 30–40% of the cells and produced much higher proportions of cells with small upslope contributing areas compared to the FD8 and DEMON MFD algorithms. The results also showed that the choice of cross-grading area threshold, which is utilized in TAPES-G to switch from FD8 to D8, produced very small differences (<5%) in upslope contributing and specific catchment area values. Overall, the results showed that the two MFD algorithms agreed with each other in 71% of the grid cells and that the other algorithms agreed with each other in 49–57% of the pairwise comparisons.

Chirico *et al.* (2005) evaluated several different methods for defining flow width on grids when computing SCA in the second study. Five approaches – D8 with flow width equal to grid size regardless of cell flow direction; modified D8 (D8_v1) with flow width equal to grid size for cardinal flow directions and grid size times √2 for diagonal flow directions; modified D8 (D8_v2) with flow width equal to grid size for cardinal flow directions and grid size times 1√2 for diagonal flow directions; D∞ with flow width equal to grid size regardless of cell flow direction; and modified D∞ (D∞_v1) with flow width varying as a function of flow direction – were tested on sloping planes, inward and outward cones and then compared with theoretical SCA values. Two dimensionless parameters – the global resolution, defined as the ratio of a characteristic length of the study area to the grid size, and the upslope area resolution, defined as the ratio of the local theoretical SCA to the grid size – were used to evaluate the performance of the five approaches. The results, cast in terms of the pattern of errors (i.e. absolute bias, mean absolute error, and local relative error) across different grid sizes indicated that D8 and D∞ performed better than the modified D8 and D∞ algorithms in calculating SCAs.

The second group of studies comparing the performance of two or more of the flow routing algorithms examined their ability to reproduce the drainage structure and/or some other topographic attribute. Desmet and Govers (1996), for example, evaluated six flow routing algorithms in terms of their ability to: (1) reproduce the main structure of the catchment; and (2) predict the location of ephemeral gullies. The D8 and Rho8 SFD routing algorithms produced different spatial and statistical patterns from each other and two pairs of MFD algorithms – the MFD algorithms of Quinn *et al.* (1991) and Freeman (1991), both of which allocate flow to up to eight neighbouring cells, and the ANSWERS (Beasley and Huggins 1978) and flux decomposition (Desmet and Govers 1996) algorithms, which allocate flow to one or two downslope neighbours – for their small study site in Flanders, Belgium. The MFD algorithms produced much smoother images compared to the SFD algorithms (similar to Wolock and McCabe 1995) and taken as a whole, Desmet and Govers (1996) favoured the two algorithms that allowed flow to only one or two downslope neighbours because they (visually) produced a stronger correlation with the main drainage lines. The main structure of the catchment (i.e. the interfluves and main drainage lines) was identified by all six flow direction algorithms and most of the variability occurred in higher elevation areas (based on the maps reproduced in the manuscript).

Desmet and Govers (1996) also examined the effect of the choice of flow direction algorithm on the prediction of ephemeral gullies identified using the methodology of Moore *et al.* (1988). Their results showed that the MFD algorithms were able to identify areas where ephemeral gully erosion is likely, but they could not predict the precise location of the gullies (which never exceeded half the width of the grid cells for this particular study area). The SFD algorithms predicted ephemeral gullies to start higher on the slopes but the correspondence with observed patterns was erratic because these algorithms were very sensitive to small elevation errors.

Zhou and Liu (2002) computed "true" SCAs for ellipsoid, inverse ellipsoid, saddle, and planar simulated surfaces and compared these values to the SCAs derived from the D8, Rho8, Freeman (1991), DEMON, and D∞ flow routing algorithms. The accuracy and spatial distribution of residuals were also analysed by calculating the Root Mean Square Error, mean error, and standard deviation. They found that DEMON generated the lowest randomly distributed error values across all surfaces. Qin *et al.* (2007) used the same simulated surfaces and statistics to compare the performance of their new MFD-md algorithm with D8 and a derivative of the MFD algorithm of Quinn *et al.* (1991). Their results showed that MFD-md produced the lowest error amongst the three algorithms across all four simulated surfaces.

Wilson *et al.* (2007) compared the performance of pairs of SCA grids computed from five flow routing algorithms (D8, Rho8, FD8, DEMON, and D∞) across six user-defined fuzzy landscape classes. Table 1a lists the basic SCA statistics by flow routing algorithm. The minimum values varied because different rules were used to direct flow from each source cell to one or more adjacent downslope cells. The maximum values are similar because they represent watershed outlets at the coast. The mean values varied from a low of 3,429 m^2m^{-1} (DEMON) to a high of 4,356 m^2m^{-1} (FD8), a difference of 27%. Table 1b partitions SCA into a series of classes and indicates the percentage of cells for each flow routing algorithm that was assigned to each class. These results show that D8 and Rho8, and to a lesser extent D∞, have many more "low flow" cells (i.e. SCA $\leq$ 10 m^2 m^{-1}). The same pattern is repeated for the second class although the magnitude of the differences is reduced. The largest number of cells in classes 3 through 6 was generated with different flow routing algorithms – D∞ for class 3, DEMON for class 4, and FD8 for the fifth and sixth classes – although the differences are relatively small.

Table 1. (a) Specific catchment area ($m^2 m^{-1}$) statistics for study area, and (b) percentage of cells per specific catchment area class.

(a)	*Number of cells*	*Minimum*	*Maximum*	*Mean*	*Standard Deviation*
D8	1,263,296	7.07	2237670.25	3715.27	60584.28
Rho8	1,263,296	7.07	2236030.25	3714.18	60469.64
D∞	1,263,296	10.00	2236762.00	3934.18	61469.07
FD8	1,263,296	2.56	2341777.00	4355.83	69911.69
DEMON	1,263,296	7.07	2214353.00	3428.91	55657.18

(b)	*SCA Classes (m^2m^{-1})*						
	1 (≤10.0)	2 (10.1-20)	3 (20.1-40)	4 (40.1-70)	5 (70.1-100)	6 (100.1-1000)	7 (>1000)
D8	12.8	18.5	26.9	16.3	7.2	13.3	5.1
Rho8	13.4	21.6	25.0	14.3	6.7	14.0	5.1
D∞	7.6	12.9	29.9	20.1	7.9	16.0	5.7
FD8	4.5	12.1	24.5	20.7	10.0	23.2	5.2
DEMON	2.7	12.2	29.3	23.6	9.6	17.6	5.0

Table 2 summarizes several noteworthy features about the distribution of low flow cells predicted with the five flow algorithms across the six landscape classes. First, the number of low flow cells predicted with the five flow routing algorithms varied from 169,171 (Rho8) to 33,756 (DEMON). Second, the percentage of low flow cells in the hilltop/ridgeline class varied by a factor of five, from a low of 9% for DEMON to a high of 45% for D8. In general, these percentages indicate the presence of a series of broad hilltops and ridgelines in the study area. Third, Rho8 predicted > 5,000 low flow cells in five of the six landscapes and D8 predicted > 5,000 low flow cells for steep north-facing slopes. Neither of these results is realistic. Overall, the results show that D∞, FD8, and DEMON performed better than D8 and especially Rho8 – the latter algorithm, in particular, had large numbers of low flow cells scattered across most of the fuzzy *k*-means landscape classes – and that the algorithms produced different results in different parts of the catchment.

The final pair of studies that comprise the third group are noteworthy because they compared the performance of the flow routing algorithms to observations of soil wetness and overland flowpaths. Fried *et al.* (2000) estimated the topographic wetness index with four flow routing approaches (static D8 and DEMON, as described in the previous section, and two quasi-dynamic versions of D8, one with dynamic uniform soils and the other with dynamic variable soils) and evaluated the resultant models using field data collected during a post-storm event GPS survey of ponded storm flow accumulations and concentrated storm flow discharge sites for a small first-order catchment in Michigan. The results showed that the quasi-dynamic versions of D8 calculated with DYNWET (Barling *et al.* 1994; see next section for additional discussion of this approach) performed best and that the areas of greatest disagreement were relatively flat, lending credence to the conventional wisdom that flowpath determination by any method is especially challenging in areas of low relief (see Callow *et al.* (2007) for additional insights).

Table 2. Distribution of source cells (SCA ≤ 10 m^2m^{-1}) by landscape class.

Topo-climatic Class	Number of Cells	Percentage of Cells with SCA ≤ 10 m^2m^{-1}				
		D8	Rho8	D∞	FD8	DEMON
Hilltops/ ridgelines	256,012	114,186	79,789	64,966	39,215	23,583
		(44.6%)	(31.2%)	(25.4%)	(15.3%)	(9.2%)
Steep south-facing slopes	323,989	1,686	25,568	481	107	91
		(0.5%)	(7.9%)	(0.1%)	(0.0%)	(0.0%)
Steep north-facing slopes	231,180	5,630	18,584	331	72	86
		(2.4%)	(8.0%)	(0.1%)	(0.0%)	(0.0%)
Moderately steep lower valley slopes	169,173	37	8,245	175	15	9
		(0.0%)	(4.9%)	(0.1%)	(0.0%)	(0.0%)
Coastal plains /gentle slopes	177,787	39,893	36,526	28,995	16,709	9,960
		(22.4%)	(20.5%)	(16.3%)	(9.4%)	(5.6%)
Stream channels	103,888	35	459	94	62	27
		(0.0%)	(0.4%)	(0.1%)	(0.1%)	(0.0%)
Total Area	1,262,029	161,467	169,171	95,042	56,180	33,756
		(12.8%)	(13.4%)	(7.5%)	(4.5%)	(2.7%)

Endreny and Woods (2003) compared the spatial congruence of observed overland flow paths with those delineated using the D8, FD8, 2D-Lea, 2D-Jensen (Jensen 1996), and D∞ algorithms on agricultural hillslopes in New Jersey. Four new algorithms were created to determine whether the congruence between observed and simulated flow networks improved with changes in the method for allocating flow about the path of steepest descent. D8-buf allowed flow to disperse into all adjacent downslope cells inside a user-specified buffer; D8-2x allowed flow to be split between two downslope cells at the source pixel and then each flow path followed the path of steepest descent; whereas MF(5) and MF(3) constrained the eight possible flow paths available in the FD8 algorithm to the five and three adjacent downslope cells with the steepest gradients, respectively. The results suggest using flow routing algorithms that disperse flow to two or three neighbouring cells when routing runoff across the landscape. The favoured algorithms included D8-buf and MF(3) along with the more sophisticated 2D-Lea, 2D-Jenson, and D∞ algorithms since all five of these algorithms produced the best spatial congruence and kept the commission and omission errors at very low levels.

4 Discussion and Conclusions

It is clear from the aforementioned evaluations that the nine flow routing algorithms produce different results from one another and that the differences can be expected to vary in different parts of the landscape. The nine algorithms take different approaches to fitting a surface to the square-grid DEMs and in terms of the rationale and number of cells to which flow is apportioned. These algorithms all treat flow routing as a function of the topographic surface despite the likelihood that this is only true in a series of relatively rare special cases (i.e. when a land surface is impermeable). The evaluations are noteworthy in that only two studies compared the performance of these algorithms to observations. Both of these studies relied on visual (i.e. qualitative) assessments and recommended using specific algorithms based on "goodness-of-fit" without resort to any theory or knowledge of the soil water relationships that help to direct runoff across the landscape. This is a fundamental shortcoming because the successful deployment of these flow routing algorithms in watershed modelling applications depends ultimately on the amount of spatial variability they are able to reliably measure or account for (Western *et al.* 1999).

Various authors have identified the influence of interpolation errors in DEMs and their propagation through the computation of flowpaths and topographic indices to model output (Desmet 1997, Heuvelink and Goodchild 1998, Holmes *et al.* 2000, McMaster 2002, Van Niel *et al.* 2004). However, while terrain and errors in modelled terrain play an important role in the spatial distribution of surface processes, the spatial patterns of these processes may vary substantially because of the variability of soil and land cover characteristics. Mitas and Mitasova (1998), for example, found that borders between different land cover types (e.g. bare soil and dense grass) caused abrupt changes in flow velocities as well as in transport and detachment capacities, creating effects important for erosion prevention. Management actions may also modify flowpaths since cross-slope furrows tend to channel overland flow directly into concavities, leading to significant flow convergence at points upslope of those that would be identified on the grounds of topography alone (Brown and Quine 1999). There is clearly a need to consider the spatial variability of numerous factors in addition to terrain shape, as illustrated by the example below.

Zhu and Mackay (2001) investigated the effect of using detailed SoLIM spatial soil data in place of traditional soil map data as an input to both lumped and spatially distributed runs of the RHESSys model (Tague and Band 2001). RHESSys is designed to represent surface soil, topographic, and vegetation patterns along with certain hydro-ecological processes at the landscape level, so that the necessary parameters can be realistically estimated to reproduce the dominant patterns of hydro-ecological dynamics (e.g. surface runoff, evapotranspiration, canopy photosynthesis) over the landscape (Band *et al.* 1993). The SoLIM result map described the spatial variation of hydraulic conductivity by identifying contrasts between north and south facing slopes, and between high and low elevations due to the level of soil profile development, thereby providing details that were not visible on traditional soil maps.

The implications of ineffective representation of the spatial details of soil depth and hydraulic conductivity were highlighted when Zhu and Mackay (2001) ran various hydro-ecological models within RHESSys using the detailed (SoLIM) and conventional soil data as input. Underestimation of solum depth using the traditional soil map led to the soils responding quickly and abruptly to precipitation events, producing a rapidly changing and generally unrealistic hydrograph. The soil profile was thus predicted to saturate with less precipitation, while overestimation of hydraulic conductivity simulated water to move too rapidly through the soil column. In the SoLIM scheme, however, soil conditions on side slopes and their deviation from the dominant soil type were considered in model parameterization, and as a result the peaks of the simulated hydrograph were lower and more sensibly characterized the hydrologic response. Interestingly, the simulated streamflow between the two different soil landscape parameterization schemes was small under the distributed approach. Zhu and Mackay (2001) argue this is due to local variation of soil properties (solum depth and hydraulic conductivity) being expressed by the detailed description of other landscape parameters in the distributed approach, particularly the spatial covariation of local topography (elevation and slope gradient) and drainage area on a hillslope.

The spatial variability of soil and land cover characteristics is important because the location and extent of variable source areas is determined by the antecedent soil water content and its spatial distribution within the catchment in many environments (e.g. Walter *et al.* 2007). We therefore need to be able to characterize the spatial variability of soil water content in a simple, yet physically realistic way to generate meaningful hydrologic predictions at the catchment scale (Moore *et al.* 1993). Most models and applications rely on the topographic wetness index ($\ln(A_s/\tan\beta)$) to characterize the soil water distribution, although this form of the wetness index will only serve as a good predictor of soil water content if the drainage flux has reached steady state (i.e. if every point is experiencing drainage from its entire upslope contributing area) (Barling *et al.* 1994).

This last assumption is not true in many watersheds for at least part of the year because the velocity of subsurface flow is so small that most points in a catchment only receive contributions from a small part of their total upslope contributing area and the subsurface flow regime is in a state of dynamic non-equilibrium. Barling *et al.* (1994) proposed a quasi-dynamic wetness index ($\ln(A_e/\tan\beta)$), where A_e is the effective specific catchment area and β is the slope angle, and showed that this approach was a better predictor of soil water content for a small catchment near Wagga Wagga in New South Wales, Australia. This approach, which requires the user to specify drainage times and two soil properties (saturated hydraulic conductivity and drainable porosity), is novel because they considered soil properties in addition to the shape of the topographic surface.

More work along these lines is needed because hydrologic applications utilize flow routing algorithms to connect the precipitation falling on the land surface with the hydrologic response of the catchment. This work will require a greater investment in fieldwork and data modelling than is evident from the flow routing papers published during the past two decades. We need better data models to get the runoff from the land surface to the stream networks (see Kim and Lee 2004 for one such example) and most important of all, we will need field observations in a variety of landscape settings to improve our characterization of the role of topography, soil, and land cover in shaping the hydrologic response of catchments.

References

Abbott, M.B. and Refsgaard, J.C. (eds.), (1996), *Distributed Hydrological Modelling,* Norwell, MA: Kluwer.

Band, L.E., (1989), A terrain-based watershed information system, *Hydrological Processes,* **3**:151–162.

Band, L.E., Patterson, P., Nemani, R. and Running, S.W., (1993), Forest ecosystem processes at the watershed scale: Incorporating hillslope hydrology, *Agriculture, Forestry and Meteorology,* **63:** 93–126.

Barling, R.D., Moore, I.D. and Grayson, R.B., (1994), A quasi-dynamic wetness index for characterizing the spatial distribution of zones of surface saturation and soil water content, *Water Resources Research,* **30:** 1029–1044.

Beasley, D.G. and Huggins, L.F., (1978), ANSWERS: A model for watershed planning, *Proceedings of the Tenth Conference on Water Simulation (Volume 2),* Miami Beach, Florida: 507–515.

Beven, K.J., (ed.), (1998), Distributed Hydrological Modelling: Applications of the TOPMODEL Concept, Chichester: John Wiley and Sons.

Beven, K.J., Lamb, R., Quinn, P., Romanowicz, R. and Freer, J., (1994), TOPMODEL, In Singh, V.P. (ed.): *Computer Models of Watershed Hydrology,* Fort Collins, CO: Water Resources Publications: 627–668.

Brown, A.G. and Quine, T.A., (1999), Fluvial processes and environmental change: An overview. In Brown, A.G. and Quine, T.A. (eds.): *Fluvial Processes and Environmental Change,* Chichester: John Wiley and Sons: 1–28.

Callow J.N., Van Niel, K.P. and Boggs, G.S., (2007), How does modifying a DEM to reflect known hydrology affect subsequent terrain analysis? *Journal of Hydrology,* **332**: 30–39.

Carrara, A., Bitelli, G. and Carla, R., (1997), Comparison of techniques for generating digital terrain models from contour lines, *International Journal of Geographical Information Science,* **11:** 451–473.

Chirico, G.B., Western, A.W., Grayson, R.B. and Günter, B., (2005), On the definition of the flow width for calculating specific catchment area patterns from gridded elevation data, *Hydrological Processes,* **19:** 2539–2556.

Cluis, D., Martz, L., Quentin, E. and Rechatin, C., (1996), Coupling GIS and DEMs to classify the Hortonian pathways of non-point sources to the hydrographic network, In Kovar, K. and Nachtnebel, H.P., (eds.): *HydroGIS '96: Application of Geographic Information Systems in Hydrology and Water Resources Management (Proceedings of the Vienna Conference, (1996),* Wallingford: International Association of Hydrological Sciences: 37–44.

Costa-Cabral, M.C. and Burgess, S.J., (1994), Digital Elevation Model Networks (DEMON): A model of flow over hillslopes for computation of contributing and dispersal areas, *Water Resources Research,* **30:** 1681–1692.

Da Ros, D. and Borga, M., (1997), Use of digital elevation model data for the derivation of the geomorphological instantaneous unit hydrograph, *Hydrological Processes,* **11:** 13–33.

Desmet, P.J.J., (1997), Effects of interpolation errors on the analysis of DEMs, *Earth Surface Processes and Landforms,* **22:** 563–580.

Desmet, P.J.J. and Govers, G., (1996), Comparison of routing algorithms for digital elevation models and their implications for predicting ephemeral gullies, *International Journal of Geographical Information Systems,* **10:** 311–331.

Dymond, J.R., Derose, R.C. and Harmsworth, G.R., (1995), Automated mapping of land components from digital elevation data, *Earth Surface Processes and Landforms,* **20:** 131–137.

Eastman, J.R., (1992), *IDRISI (Version 4.0): Geographic Information System Software and Documentation,* Worcester, MA: Clark University Graduate School of Geography.

Eklundh, L. and Martensson, U., (1995), Rapid generation of digital elevation models from topographic maps, *International Journal of Geographical Information Systems,* **9:** 329–340.

Endreny, T.A. and Woods, E.W., (2003), Maximizing spatial congruence of observed and DEM-delineated overland flow networks, *International Journal of Geographic Information Science,* **17,** 699–713.

Fairfield, J. and Leymarie, P., (1991), Drainage networks from grid digital elevation models, *Water Resources Research,* **27:** 709–717.

Freeman, G.T., (1991), Calculating catchment area with divergent flow based on a regular grid, *Computers and Geosciences,* **17:** 413–422.

Fried, J.S., Brown, D.G., Zweifler, M.O. and Gold, M.A., (2000), Mapping contributing areas for stormwater discharge to streams using terrain analysis, In Wilson, J.P. and Gallant, J.C., (eds.): *Terrain Analysis: Principles and Applications,* New York: John Wiley and Sons: 183–203.

Gallant, J.C. and Wilson, J.P., (1996), TAPES-G: A grid-based terrain analysis program for the environmental sciences, *Computers and Geosciences,* **22:** 713–722.

Gallant, J.C. and Wilson, J.P., (2000), Primary terrain attributes, In Wilson, J.P. and Gallant, J.C., (eds.): *Terrain Analysis: Principles and Applications,* New York: John Wiley and Sons: 51–85.

Gallant, J.C., Hutchinson, M.F. and Wilson, J.P., (2000), Future directions for terrain analysis, In Wilson, J.P. and Gallant, J.C., (eds.): *Terrain Analysis: Principles and Applications,* New York: John Wiley and Sons: 423–427.

Garbrecht, J. and Martz, L.W., (1997), The assignment of drainage directions over flat areas in raster digital elevation models, *Journal of Hydrology,* **193:** 204–213.

Garbrecht, J., Ogden, F.L., DeBarry, P.A. and Maidment, D.R., (2001), GIS and distributed watershed models: I, Data coverages and sources, *Journal of Hydrologic Engineering,* **6:** 506–514.

Hellweger, R., (1996), *Agree.aml,* Austin, TX: Centre for Research in Water Resources, University of Texas.

Heuvelink, G. and Goodchild, M.F., (1998), *Error Propagation in Environmental Modelling with GIS,* London: Taylor and Francis.

Holmes, K.W., Chadwick, O.A. and Kyriakidis, P.C., (2000), Error in a USGS 30-meter digital elevation model and its impact on terrain modelling, *Journal of Hydrology,* **233**: 154–173.

Holmgren, P., (1994), Multiple flow direction algorithms for runoff modelling in grid-based elevation models: An empirical evaluation, *Hydrological Processes,* **8:** 327–334.

Hutchinson, M.F., (1989), A new procedure for gridding elevation and stream line data with automatic removal of pits, *Journal of Hydrology,* **106:** 211–232.

Hutchinson, M.F., (2007), Adding the Z Dimension, In Wilson, J.P. and Fotheringham, A.S., (eds.): *Handbook of Geographic Information Science,* Oxford: Blackwell: 144–68.

Jensen, J.R., (1996), Introductory Digital Image Processing: A Remote Sensing Perspective, Upper Saddle Creek, NJ: Prentice-Hall.

Kemp, K.K., (1997a), Fields as a framework for integrating GIS and environmental process models: I, Representing spatial contiguity, *Transactions in GIS,* **1:** 219–234.

Kemp, K.K., (1997b), Fields as a framework for integrating GIS and environmental process models: II, Specifying field variables, *Transactions in GIS,* **1:** 235–246.

Kim, S. and Lee, H. (2004), A digital elevation analysis: A spatially distributed flow apportioning algorithm, *Hydrological Processes,* **18:** 1777–1794.

Knighton, D., (1998), *Fluvial Forms and Processes,* New York: Oxford University Press.

Krajewski, S.A. and Gibbs, B.L., (1994), Computer contouring generates artefacts, *Geotimes,* **39:** 15–19.

Lagacherie, P., Moussa, R., Cormary, D. and Molenat, J., (1996), Effects of DEM data source and sampling pattern on topographical parameters and on a topography-based hydrological model, In Kovar, K. and Nachtnebel, H.P., (eds.): *HydroGIS '96: Application of Geographic Information Systems in Hydrology and Water Resources Management (Proceedings of the Vienna Conference, (1996),* Wallingford: International Association of Hydrological Sciences): 191–199.

Lea, N.L., (1992), An aspect driven kinematic routing algorithm. In Parsons, A.J. and Abrahams, A.D., (eds.): *Overland Flow: Hydraulics and Erosion Mechanics,* London: UCL Press: 393–407.

Lee, J. and Chu, C.-J., (1996), Spatial structures of digital terrain models and hydrological feature extraction. In Kovar, K. and Nachtnebel, H.P., (eds.): *HydroGIS '96: Application of Geographic Information Systems in Hydrology and Water Resources Management (Proceedings of the Vienna Conference, (1996),* Wallingford: International Association of Hydrological Sciences: 201–6.

Liu, H. and Jezek, K.C., (1999), Investigating DEM error patterns by directional variograms and Fourier analysis, *Geographical Analysis,* **31:** 249–266.

Lopez, C., (1997), Locating some types of random errors in digital terrain models, *International Journal of Geographical Information Science,* **11:** 677–698.

Maidment, D., (1996), Environmental modelling with GIS, In Goodchild, M.F., Steyaert, L.T. and Parks B.O. (eds.): *GIS and Environmental Modelling: Progress and Research Issues,* Fort Collins, CO: GIS World Books: 315–23.

McMaster, K.J., (2002), Effects of digital elevation model resolution on derived stream network positions, *Water Resources Research,* **38**: 13–19.

Mitas, L. and Mitasova, H., (1998), Distributed soil erosion simulation for effective erosion prevention, *Water Resources Research,* **34:** 505–516.

Montgomery, D.R. and Dietrich, W.E., (1988), Where do channels begin? *Nature,* **336:** 232–234.

Montgomery, D.R., Dietrich, W.E. and Sullivan, K., (1998), The role of GIS in watershed analysis, In Lane, S.N., Chandler, J.H. and Richards, K.S., (eds.): *Landform Monitoring, Modelling, and Analysis,* Chichester: John Wiley and Sons: 241–262.

Moore, I.D., (1996), Hydrologic modelling and GIS, In Goodchild, M.F., Steyaert, L.T., Parks, B.O., Johnston, C., Maidment, D., Crane, M. and Glendinning, S., (eds.): *GIS and Environmental Modelling: Progress and Research Issues,* Fort Collins, CO: GIS World Books: 143–148.

Moore, I.D., Burch, G.J. and MacKenzie, D.H., (1988), Topographic effects on the distribution of surface soil water and the location of ephemeral gullies, *Trans. of the American Society of Agricultural Engineers,* **31:** 1098–1107.

Moore, I.D., Grayson, R.B. and Ladson, A.R., (1991), Digital terrain modelling: A review of hydrological, geomorphological, and biological applications, *Hydrological Processes,* **5:** 3–30.

Moore, I.D., Turner, A.K., Wilson, J.P., Jenson, S.K. and Band, L.E., (1993), GIS and land surface-subsurface modelling, In Goodchild, M.F., Parks, B.O. and Steyaert, L.T. (eds.): *Environmental Modelling with GIS,* New York: Oxford University Press: 196–230.

Murillo, M. and Hunter, G.J., (1997), Assessing uncertainty due to elevation error in a landslide susceptibility model, *Transactions in GIS,* **2:** 289–298.

O'Callaghan, J.F. and Mark, D.M., (1984), The extraction of drainage networks from digital elevation data, *Computer Vision, Graphics and Image Processing,* **28:** 328–344.

Pickup, G. and Chewings, V.H., (1996), Correlations between DEM-derived topographic indices and remotely-sensed vegetation cover in rangelands, *Earth Surface Processes and Landforms,* **21,** 517–529.

Qian, J., Ehrich, R.W. and Campbell, J.B., (1990), DNESYS: An expert system for automatic extraction of drainage networks from digital elevation data, *IEEE Transactions on Geoscience and Remote Sensing,* **28:** 29–45.

Qin, C., Zhu, A.-X., Pei, T., Li, B., Zhou, C. and Yang, L., (2007), An adaptive approach to selecting flow partition exponent for multiple flow direction algorithm, *International Journal of Geographical Information Science,* **21:** 443–458.

Quinn, P.F., Beven, K.J., Chevallier, P. and Planchon, O., (1991), The prediction of hillslope flow paths for distributed hydrological modelling using digital terrain models, *Hydrological Processes,* **5,** 59–79.

Quinn, P.F., Beven, K.J. and Lamb, R., (1995), The ln(a/tanβ) index: How to calculate it and how to use it within the TOPMODEL framework, *Hydrological Processes,* **9:** 161–182.

Smith, T.R., Zhun, X. and Gan, P., (1990), A knowledge-based, two-step procedure for extracting channel networks from noisy DEM data, *Computers and Geosciences,* **16:** 777–786.

Storck, P., Bowling, L., Wetherbee, P. and Lettenmaier, D., (1998), Application of a GIS-based distribution hydrology model for prediction of forest harvest effects on peak stream flow in the Pacific Northwest, *Hydrological Processes,* **12:** 889–904.

Tague, C. and Band, L.E., (2001), Evaluating explicit and implicit routing for watershed hydro-ecological models of forest hydrology at the small catchment scale, *Hydrological Processes,* **15:** 1415–1439.
Tarboton, D.G., (1997), A new method for the determination of flow directions and upslope areas in grid digital elevation models, *Water Resources Research,* **33:** 309–319.
Van Niel, K.P., Laffan, S.W. and Lees, B.G., (2004), Effect of error in the DEM on environmental variables for predictive vegetation modelling, *Journal of Vegetation Science,* **15:** 747–756.
Walter, M.T., Walter, M.F., Brooks, E.S., Steenhuis, T.S., Boll, J. and Weiler, K., (2007), Hydrologically sensitive areas: Variable source area hydrology implications for water quality risk assessment, *Journal of Soil and Water Conservation,* **62:** 277–284.
Western, A.W., Grayson, R.B., Bloschl, G., Willgoose, G.R. and McMahon, M.L., (1999), Observed spatial organization of soil moisture and its relation to terrain indices., *Water Resources Research,* **35:** 797–810.
Wilson, J.P. and Gallant, J.C., (2000), Digital terrain analysis, In Wilson, J.P.and Gallant, J.C., (eds.): *Terrain Analysis: Principles and Applications,* New York: John Wiley and Sons: 1–27.
Wilson, J.P., Lam, C.S. and Deng, Y.X., (2007), Comparison of performance of flow-routing algorithms used in Geographic Information Systems, *Hydrological Processes,* **21:** 1026–1044.
Wilson, J.P., Repetto, P.L. and Snyder, R.D., (2000), Effect of data source, grid resolution, and flow-routing method on computed topographic attributes, In Wilson, J.P. and Gallant, J.C., (eds.):*Terrain Analysis: Principles and Applications*, New York: John Wiley and Sons: 133–61.
Wilson, J.P., Spangrud, D.S., Nielsen, G.A., Jacobsen, J.S. and Tyler, D.A., (1998), GPS sampling intensity and pattern effects on computed terrain attributes., *Soil Science Society of America Journal,* **62:** 1410–1417.
Wise, S.M. (1998a), The effect of GIS interpolation errors on the use of digital elevation models in geomorphology, In Lane, S.N., Richards, K.S. and Chandler, J.H., (eds.):*Landform Monitoring, Modelling, and Analysis,* New York: John Wiley and Sons: 139–64.
Wise, S.M., (1998b), Digital terrain models: Traps for the unwary, *Proceedings of the Third International Conference on GeoComputation, University of Bristol, United Kingdom,* Available online at: http://www.geog.port.ac.uk/geocomp/geo98/ (accessed 1 September 2007).
Wolock, D.M. and McCabe, G.J., (1995), Comparison of single and multiple flow direction algorithms for computing topographic parameters in TOPMODEL, *Water Resources Research,* **31:** 1315–1324.
Zhou, Q. and Liu, X., (2002), Error assessment of grid-based flow routing algorithms used in hydrological models, *International Journal of Geographical Information Science,* **16:** 819–842.
Zhu, A-X. and Mackay, D.S., (2001), Effects of spatial detail of soil information on watershed modelling, *Journal of Hydrology,* **248:** 54–77.